

See discussions, stats, and author profiles for this publication at: <https://www.researchgate.net/publication/257954446>

# Exciton-plasmon coupling mediated photorefractivity in gold-nanoparticle- and quantum-dot-dispersed polymers

ARTICLE *in* APPLIED PHYSICS LETTERS · JUNE 2013

Impact Factor: 3.3 · DOI: 10.1063/1.4812720

---

CITATIONS

3

---

READS

42

5 AUTHORS, INCLUDING:



**Chengmingyue Li**

Washington University in St. Louis

13 PUBLICATIONS 26 CITATIONS

SEE PROFILE



**Xiangping Li**

Jinan University (Guangzhou, China)

71 PUBLICATIONS 526 CITATIONS

SEE PROFILE



**Liangcai Cao**

Tsinghua University

103 PUBLICATIONS 526 CITATIONS

SEE PROFILE

## Exciton-plasmon coupling mediated photorefractivity in gold-nanoparticle- and quantum-dot-dispersed polymers

Chengmingyue Li, Xiangping Li, Liangcai Cao, Guofan Jin, and Min Gu

Citation: *Appl. Phys. Lett.* **102**, 251115 (2013); doi: 10.1063/1.4812720

View online: <http://dx.doi.org/10.1063/1.4812720>

View Table of Contents: <http://apl.aip.org/resource/1/APPLAB/v102/i25>

Published by the AIP Publishing LLC.

---

### Additional information on Appl. Phys. Lett.

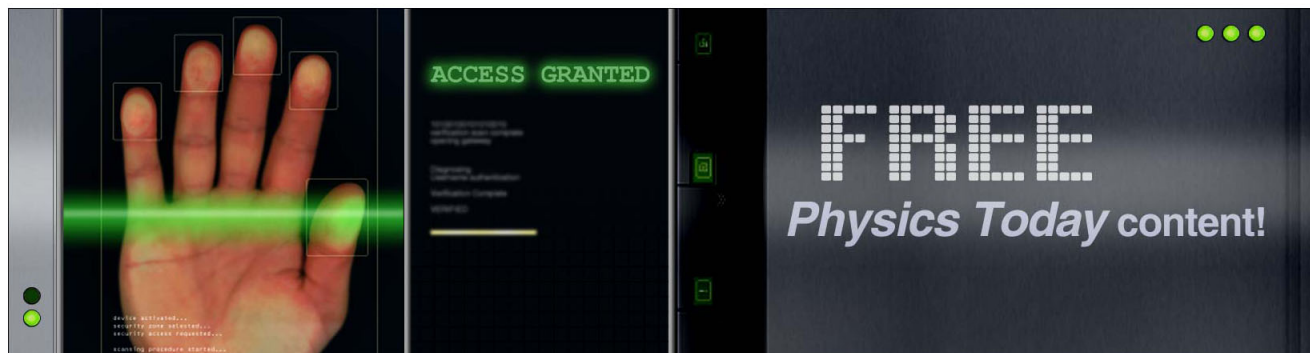
Journal Homepage: <http://apl.aip.org/>

Journal Information: [http://apl.aip.org/about/about\\_the\\_journal](http://apl.aip.org/about/about_the_journal)

Top downloads: [http://apl.aip.org/features/most\\_downloaded](http://apl.aip.org/features/most_downloaded)

Information for Authors: <http://apl.aip.org/authors>

## ADVERTISEMENT



# Exciton-plasmon coupling mediated photorefractivity in gold-nanoparticle- and quantum-dot-dispersed polymers

Chengmingyue Li,<sup>1,2</sup> Xiangping Li,<sup>1,a)</sup> Liangcai Cao,<sup>2</sup> Guofan Jin,<sup>2</sup> and Min Gu<sup>1,a)</sup>

<sup>1</sup>Centre for Micro-Photonics, Faculty of Engineering and Industrial Sciences,  
Swinburne University of Technology, Hawthorn, Victoria 3122, Australia

<sup>2</sup>State Key Laboratory of Precision Measurement Technology and Instruments, Tsinghua University,  
Beijing 100084, China

(Received 26 May 2013; accepted 16 June 2013; published online 27 June 2013)

In this paper, we report on the enhanced photorefractivity induced by the exciton-plasmon coupling in type-II CdSe/CdTe quantum-dot (QD) and gold-nanoparticle (NP)-doped polymeric nanocomposites (NCs). The new NCs exhibit a nearly 110% increase in the refractive-index grating construction speed and a 100% enhancement in the two-beam coupling gain coefficient compared with those of QD-sensitized samples at moderate biases. These features are achieved by the exciton-plasmon coupling between QDs and Au NPs, which leads to not only an enhanced charge separation process but also a reduced recombination probability of free carriers during the charge transport. © 2013 AIP Publishing LLC. [<http://dx.doi.org/10.1063/1.4812720>]

With the capability of reversible optical manipulation of the refractive index in materials, the polymeric photorefractive (PR) effect<sup>1</sup> holds tremendous potential in the applications for real-time updatable holography and fast opto-electronic devices with a low cost and a compositional flexibility.<sup>2,3</sup> In polymers, photorefractivity arises when charge carriers, photo-generated by a spatially-inhomogeneous irradiation pattern, are separated and trapped to produce a non-uniform space-charge field for the subsequent nonlinear refractive-index modulation.<sup>4</sup> As such, incorporating semiconductor quantum dots (QDs) into PR polymers as photocharge generators has attracted intense research either to enhance the electro-optic effect of nonlinear dyes<sup>5–9</sup> or re-orientation effect of liquid crystals.<sup>10–12</sup> However, the typical PR performances of almost all QD-polymer composites have been low with slow response speeds associated with low charge separation efficiencies in QDs, and low diffraction efficiencies associated with high recombination probabilities of free carriers after the charge separation.<sup>5,13,14</sup>

Even though enormous efforts have been spent to enhance their PR performance by using surface engineered type-I and type-II core/shell QDs, limited success has been achieved at a cost of either a reduced response speed<sup>15</sup> or a restricted refractive-index modulation strength.<sup>16</sup> On the other hand, the surface plasmon in metallic nanoparticles (NPs) coupling with the exciton of QDs can dramatically enhance the subsequent photophysics of QDs,<sup>17,18</sup> opening a new approach to improve the performance of QD-based opto-electronic devices. The exciton-plasmon coupling could potentially tackle these drawbacks of PR polymers; however, its application in PR polymers has never been investigated before. Here, we report on the enhanced PR performance in Au NPs and Type-II CdSe/CdTe QD co-sensitized polymers.

In the presence of the exciton-plasmon coupling, the photogeneration in CdSe/CdTe QDs can be significantly enhanced by orders of magnitude. The possible electron transfer from

QDs to adjacent Au NPs<sup>19,20</sup> can further facilitate the photo-carrier separation, as illustrated in Fig. 1(a). This feature can dramatically improve the PR response speed, which is strongly dependent on the carrier separation process.<sup>1</sup> While the holes are scavenged by the surrounding poly(9-vinylcarbazole) (PVK), which can hop along the polymer matrix under an external bias field. Moreover, the proximal Au NPs can serve as stable electron traps owing to the electron affinity (Fig. 1(b)), and thus, the recombination probability of separated free carriers can be significantly reduced. Consequently, the overall improved PR performance in these nanocomposites (NCs) with both a fast response speed and a large diffraction efficiency becomes possible.

Type-II CdSe/CdTe QDs were prepared by using the successive ionic layer adsorption and reaction (SILAR) method.<sup>16,21</sup> Au NPs with an extinction peak at the wavelength of 530 nm and an average particle size of 45 nm were synthesized by following a well-established recipe.<sup>22</sup> Figs. 2(a) and 2(b) show the absorption spectra of QDs and Au NPs and the photoluminescence (PL) spectra of QDs with the presence of different concentrations of Au NPs. Under excitation at the wavelength of 500 nm, the PL emission of Type-II CdSe/CdTe QDs is centered around 750 nm. In Fig. 2(b), it is clear shown that the PL intensity quenching (defined as the ratio of the decrease in the PL intensity to the PL intensity without the presence of Au NPs) of QDs monotonously increases as the relative ratio of Au NPs to QDs increases. When the relative ratio of Au NPs to QDs was increased from 0 to  $5.5 \times 10^{-3}$ , the PL quenching of QDs gradually rose to more than 50%. Taking the effective excitation reduced by 15% considering the increased scattering loss at the wavelength of 500 nm by Au NPs, the observed PL quenching in the hybrid NCs indicates a reduced recombination rate and a possible electron transfer process to proximal Au NPs facilitated by the exciton-plasmon coupling.<sup>19,20</sup>

To demonstrate the exciton-plasmon coupling mediated polymeric photorefractivity, thin films of hybrid NCs were prepared by sandwiching between two indium tin oxide (ITO)-coated glass slides, following the formula of PVK:ethyl

<sup>a)</sup>Authors to whom correspondence should be addressed. Electronic addresses: xiangpingli@swin.edu.au and mgu@swin.edu.au

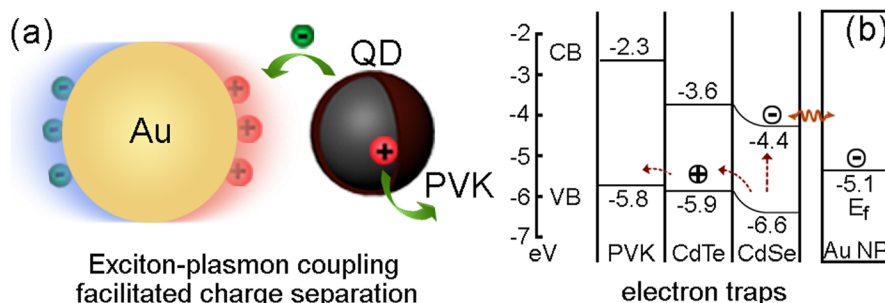


FIG. 1. (a) Scheme of the photocarrier separation facilitated by the exciton-plasmon coupling between Au NPs and type-II core/shell QDs. The electrons are rapidly transferred from QDs to proximal Au NPs while the holes are scavenged by the surrounding PVK matrix. (b) Schematic illustration of the energy levels of the hybrid NCs.  $E_f$  represents the Fermi energy level of Au NPs.

carbazole (ECZ):4-diethylaminobenzylidenemalononitrile (DABM) (Ref. 16):QDs:Au NPs at the ratio of 50 mg:20 mg:30 mg:0.1 nmol: $1.3 \times 10^{-4}$  nmol. Here, ECZ serves as the plasticizer and DABM serves as the nonlinear dye to generate the electro-optic effect. For a comparison, a controlled sample A dispersed with Au NPs and a controlled sample B dispersed with Type-II CdSe/CdTe QDs at the same concentration of the NCs sample were prepared, respectively. The mixture was dissolved into chloroform and the solution was dried at 60 °C in an oven for overnight. The dried powder was ground, and then sandwiched between two ITO glasses at 150 °C. The thickness of the thin films was controlled to be  $120 \pm 10 \mu\text{m}$  with the use of a spacer. Both four-wave mixing (FWM) and two-beam coupling (TBC) experiments were conducted at the excitation wavelength of 632.8 nm in a tilted geometry with incident angles of the two beams at 30° and 60° in air, respectively. The intensities for the two p-polarized beams were 200 and 400 mW/cm<sup>2</sup>, respectively. A two-channel detector (Newport, 2931-C) was employed to monitor the time-evolution of the transmitted intensities. It should be noted that no detectable PR performance of the sample without any sensitizer is observed.

Fig. 3(a) shows one typical example of the temporal diffraction efficiencies of the three samples obtained at the bias field of 66.7 V/ $\mu\text{m}$ . The response speed  $1/\tau$  was extracted from the initial growth of the diffracted signal by fitting the temporal diffraction curves with a biexponential equation.<sup>23</sup> The response speeds as a function of the external bias field are shown in Fig. 3(b). It reveals clearly that the PR response speeds in samples with Au NPs are much faster than that in samples without Au NPs. In addition, the response speed in the hybrid NCs is dramatically improved compared to the controlled samples. At a moderate bias field of 66.7 V/ $\mu\text{m}$ ,

the response speed in the hybrid NCs is increased 66% and 110%, compared with that of the controlled sample A sensitized by Au NPs and the controlled sample B sensitized by type-II CdSe/CdTe QDs, respectively. These results imply that the improved response speed can be largely attributed to the rapid carrier separation facilitated by the exciton-plasmon coupling.<sup>19,20</sup>

From the measured diffraction efficiencies in the FWM experiment, the strength of the refractive-index modulation  $\Delta n$  can be obtained following the Kogelnik's theory:<sup>1</sup>

$$\eta = \exp(-\alpha L) \sin^2 \left( \frac{\pi \Delta n L}{\lambda} \hat{e}_1 \cdot \hat{e}_2 \right), \quad (1)$$

where  $\lambda$  is the wavelength in the material,  $\alpha$  is the absorption coefficient,  $L$  is the effective interaction length, and  $\hat{e}_1$  and  $\hat{e}_2$  are unit vectors along the electric field of the incident and diffracted beams, respectively. The field-dependent refractive-index modulation is shown in Fig. 4(a). It depicts clearly that refractive-index modulation in the hybrid NCs are much larger than those in the controlled samples in the entire investigated field range. At the bias of 66.7 V/ $\mu\text{m}$ , a refractive-index change of  $3 \times 10^{-4}$  in the hybrid NCs was achieved, which yields a 204% and 36% enhancement, compared to the controlled sample A and the controlled sample B, respectively.

The asymmetric energy transfer in TBC experiments unambiguously confirms the observed refractive-index modulation originating from the polymeric photorefractivity.<sup>1</sup> The extracted TBC gain coefficients  $\Gamma$  as a function of the bias field is presented in Fig. 4(b). It can be seen that at the bias field of 66.7 V/ $\mu\text{m}$  the TBC coefficients in the hybrid NCs is increased by nearly 127% and 100%, compared with that in the controlled sample A and the controlled sample B,

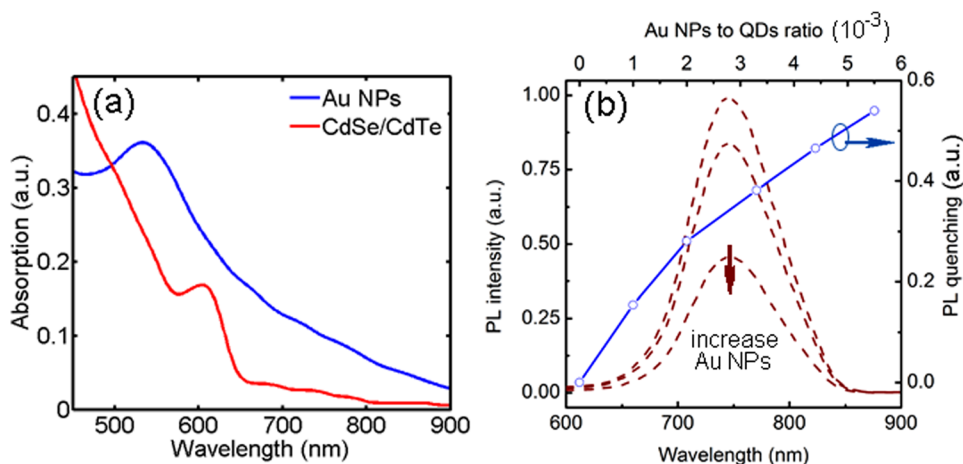


FIG. 2. (a) Absorption spectra of Type-II CdSe/CdTe QDs (red curve) and Au NPs (blue curve) in chloroform. (b) PL spectra of QDs with different concentrations of Au NPs (dashed wine curves) and the PL quenching of QDs as a function of the ratio of Au NPs to QDs (blue circles). Increasing the concentration of Au NPs (indicated by the arrow) leads to a decrease in PL intensities of QDs.

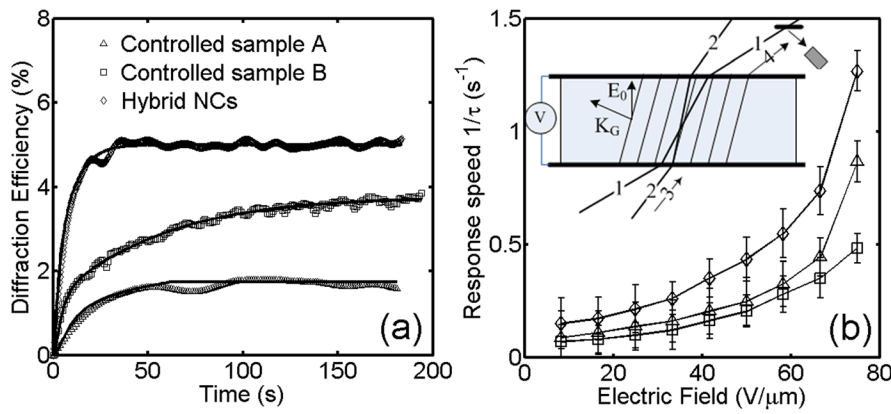


FIG. 3. (a) The temporal evolution of diffraction efficiencies at a bias field of 66.7 V/μm. (b) Response speeds as a function of the external electric field. Triangles, squares, and asterisks represent the experimental data for the controlled sample A, the controlled sample B, and the hybrid NCs, respectively. The inset shows the FWM experimental scheme. A third beam with an intensity of 9 mW/cm<sup>2</sup> was used as the probe.  $E_0$  and  $K_G$  indicate the external electric field and the intensity grating, respectively.

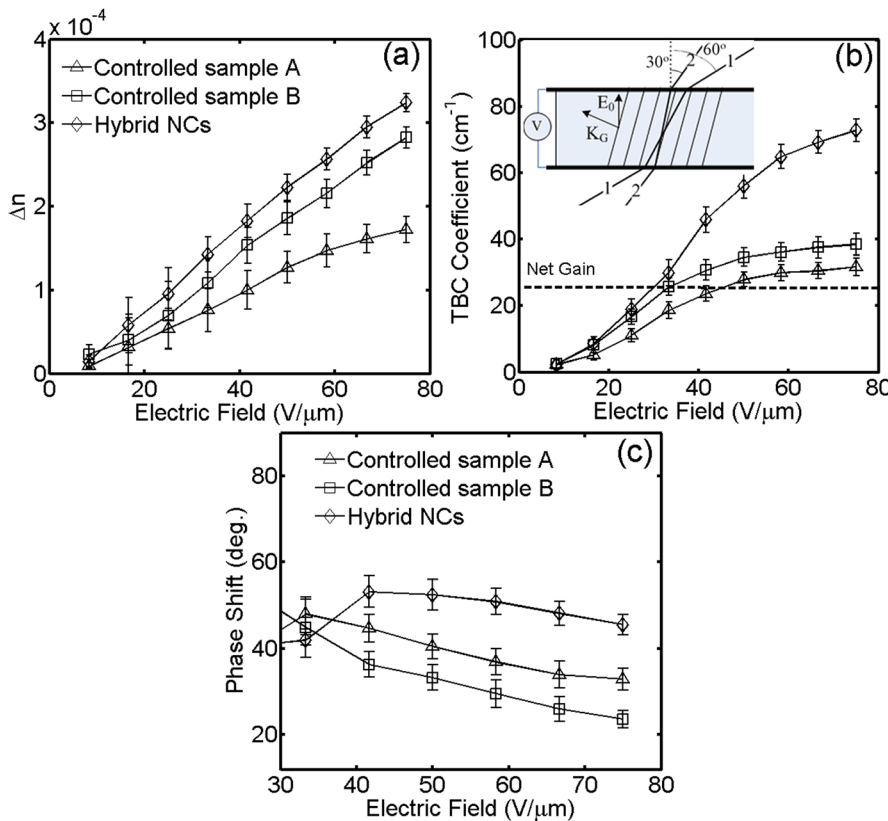


FIG. 4. Refractive-index modulation obtained from the FWM experiment (a), TBC gain coefficients (b), and phase shifts between the incident light-intensity pattern and the refractive-index grating (c) as a function of the external electric field for the controlled sample A (triangles), the controlled sample B (squares), and the hybrid NCs (asterisks). The dashed line indicates the zero net gain coefficient. The inset shows the TBC experimental scheme.  $E_0$  and  $K_G$  indicate the external electric field and the intensity grating, respectively.

respectively. To gain a better insight into the origin of the enhanced refractive-index modulation, the phase shift  $\phi_p$  between the incident light-intensity pattern and the refractive-index grating is given as<sup>1</sup>

$$\sin \phi_p = \frac{m\lambda \cdot \Gamma}{4\pi \cdot \Delta n}, \quad (2)$$

where  $\Gamma$  is the TBC gain coefficient and  $\Delta n$  is the steady-state refractive-index modulation obtained from FWM experiments;  $m = 2\sqrt{I_{1(in)}I_{2(in)}} / (I_{1(in)} + I_{2(in)})$  is the modulation depth of the writing pattern;  $I_{1(in)}$  and  $I_{2(in)}$  are the intensities of the two incident beams. The phase shifts as a function of the bias field are shown in Fig. 4(c). It is speculated that at the moderate bias fields the hybrid NCs exhibit the largest phase shifts and the controlled sample B sensitized by core/shell QDs exhibits the smallest phase shifts. The physical explanation is that Au NPs serve as electron

traps, therefore, reducing the recombination probability of free carriers during the charge transport in the polymer matrix and leading to stable space-charge fields and large phase shifts.

In conclusion, we have demonstrated the enhanced photorefractivity in the polymeric NCs sensitized by type-II CdSe/CdTe QDs and Au NPs. A nearly 100% enhanced TBC gain coefficient and a 110% enhanced response speed in the hybrid NCs sensitized by both QDs and Au NPs are achieved compared with those in the sample sensitized by QDs. Our results demonstrate the potential of developing fast and efficient opto-electronic devices using the exciton-plasmon coupling mediated photorefractivity.

This work was supported under the Australian Research Council Discovery Project scheme (DP110101422). Chengmingyue Li acknowledges the support from The Doctoral Short-term Overseas Fund of Tsinghua University.



- <sup>1</sup>W. E. Moerner, A. Grunnet-Jepsen, and C. L. Thompson, *Annu. Rev. Mater. Sci.* **27**, 585 (1997).
- <sup>2</sup>K. Meerholz, B. L. Volodin, Sandalphon, B. Kippelen, and N. Peyghambarian, *Nature* **371**, 497 (1994).
- <sup>3</sup>P. A. Blanche, A. Bablumian, R. Voorakaranam, C. Christenson, W. Lin, T. Gu, D. Flores, P. Wang, W. Y. Hsieh, M. Kathaperumal, B. Rachwal, O. Siddiqui, J. Thomas, R. A. Norwood, M. Yamamoto, and N. Peyghambarian, *Nature* **468**, 80 (2010).
- <sup>4</sup>W. E. Moerner and S. M. Silence, *Chem. Rev.* **94**, 127 (1994).
- <sup>5</sup>C. Fuentes-Hernandez, D. J. Suh, B. Kippelen, and S. R. Marder, *Appl. Phys. Lett.* **85**, 534 (2004).
- <sup>6</sup>J. G. Winiarz, L. Zhang, M. Lal, C. S. Friend, and P. N. Prasad, *J. Am. Chem. Soc.* **121**, 5287 (1999).
- <sup>7</sup>K. R. Choudhury, Y. Sahoo, and P. N. Prasad, *Adv. Mater.* **17**, 2877 (2005).
- <sup>8</sup>K. R. Choudhury, Y. Sahoo, S. Jang, and P. N. Prasad, *Adv. Funct. Mater.* **15**, 751 (2005).
- <sup>9</sup>X. Li, J. Van Embden, J. W. M. Chon, R. Evans, and M. Gu, *Appl. Phys. Lett.* **96**, 253302 (2010).
- <sup>10</sup>A. Anczykowska, S. Bartkiewicz, M. Nyk, and J. Mysliwiec, *Appl. Phys. Lett.* **101**, 101107 (2012).
- <sup>11</sup>B. Sahraoui, A. Anczykowska, S. Bartkiewicz, and J. Mysliwiec, *Opt. Express* **19**, 24454 (2011).
- <sup>12</sup>G. Cook, A. V. Glushchenko, V. Reshetnyak, A. T. Griffith, M. A. Salen, and D. R. Evans, *Opt. Express* **16**, 4015 (2008).
- <sup>13</sup>D. J. Binks, S. P. Bant, D. P. West, P. O'Brien, and M. A. Malik, *J. Mod. Opt.* **50**, 299 (2003).
- <sup>14</sup>X. Li, J. W. M. Chon, and M. Gu, *Aust. J. Chem.* **61**, 317 (2008).
- <sup>15</sup>F. Aslam, D. J. Binks, M. D. Rahn, D. P. West, P. O'Brien, and N. Pickett, *J. Mod. Opt.* **52**, 945 (2005).
- <sup>16</sup>X. Li, J. Van Embden, R. A. Evans, and M. Gu, *Appl. Phys. Lett.* **98**, 231107 (2011).
- <sup>17</sup>O. Kulakovich, N. Strekal, A. Yaroshevich, S. Maskevich, S. Gaponenko, I. Nabiev, U. Woggon, and M. Artemyev, *Nano Lett.* **2**, 1449 (2002).
- <sup>18</sup>K. Okamoto, S. Vyawahare, and A. Scherer, *J. Opt. Soc. Am. B* **23**, 1674 (2006).
- <sup>19</sup>C. W. Chen, C. H. Wang, C. M. Wei, and Y. F. Chen, *Appl. Phys. Lett.* **94**, 071906 (2009).
- <sup>20</sup>B. Nikoobakht, C. Burda, M. Braun, M. Hun, and M. A. El-Sayed, *Photochem. Photobiol.* **75**, 591 (2002).
- <sup>21</sup>B. Blackman, D. M. Battaglia, T. D. Mishima, M. B. Johnson, and X. Peng, *Chem. Mater.* **19**, 3815 (2007).
- <sup>22</sup>Y. Yang, J. Li, J. Mu, H. Rong, and L. Jiang, *Nanotechnology* **17**, 461 (2006).
- <sup>23</sup>J. G. Winiarz, *J. Phys. Chem. C* **111**, 1904 (2007).